

# Residual Squeeze-and-Excitation Network for Fast Image Deraining

Jun Fu<sup>1</sup>, Jianfeng Xu<sup>2</sup>, Kazuyuki Tasaka<sup>2</sup> and Zhibo Chen<sup>1</sup>

<sup>1</sup>University of Science and Technology of China

<sup>2</sup>KDDI Research, Inc.

fujun@mail.ustc.edu.cn, {ji-xu,ka-tasaka}@kddi-research.jp, chenzhibo@ustc.edu.cn

## Abstract

Image deraining is an important image processing task as rain streaks not only severely degrade the visual quality of images but also significantly affect the performance of high-level vision tasks. Traditional methods progressively remove rain streaks via different recurrent neural networks. However, these methods fail to yield plausible rain-free images in an efficient manner. In this paper, we propose a residual squeeze-and-excitation network called RSEN for fast image deraining as well as superior deraining performance compared with state-of-the-art approaches. Specifically, RSEN adopts a lightweight encoder-decoder architecture to conduct rain removal in one stage. Besides, both encoder and decoder adopt a novel residual squeeze-and-excitation block as the core of feature extraction, which contains a residual block for producing hierarchical features, followed by a squeeze-and-excitation block for channel-wisely enhancing the resulted hierarchical features. Experimental results demonstrate that our method can not only considerably reduce the computational complexity but also significantly improve the deraining performance compared with state-of-the-art methods.

## 1 Introduction

Outdoor images taken on rainy days often contain various rain streaks. These rain streaks not only cause noticeable degradation in scene visibility but also significantly impair the performance of advanced visual tasks, such as pedestrian detection [Liu *et al.*, 2019], object tracking [Redmon and Farhadi, 2018], and autonomous vehicles [Zang *et al.*, 2019]. Therefore, it is important and necessary to develop image deraining algorithms.

In general, a rainy image ( $I$ ) can be regarded as a linear combination of a clean background ( $B$ ) and a rain streak layer ( $R$ ):

$$I = B + R. \quad (1)$$

Image deraining aims to recover the clean background from the observed rainy image. However, due to lacking information on the rain streak layer, rain removal is a serious ill-posed problem.

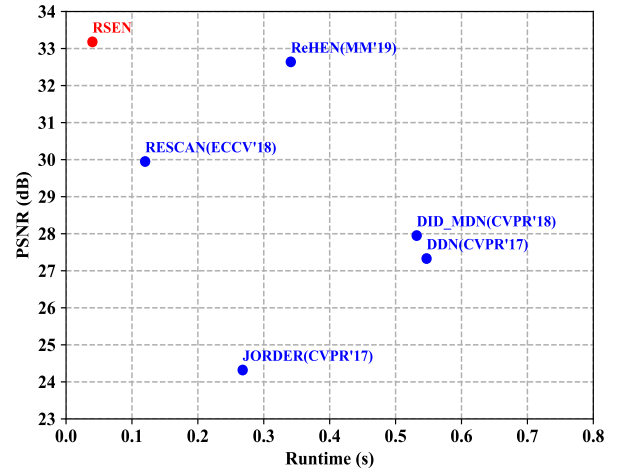


Figure 1: The PSNR-Runtime trade-off plot on the Rain1200 dataset. Compared to five state-of-the-art competitors including DDN, DID\_MDN, JORDER, RESCAN, and ReHEN, RSEN achieves superior quality and lower computational complexity.

In the past few decades, image deraining has received considerable attention from industry and academia. Existing methods can be divided into two categories, including model-driven methods and data-driven methods. Model-driven methods can be further divided into filter based ones [Xu *et al.*, 2012; Zheng *et al.*, 2013; Ding *et al.*, 2016; Kim *et al.*, 2013] and prior based ones [Luo *et al.*, 2015; Li *et al.*, 2016; Chang *et al.*, 2017]. Considering rain removal as a task of signal filtering, filter based ones utilize physical properties of rain streaks and edge-preserving filters to obtain rain-free images. However, prior based ones formulate rain removal as an optimization problem and utilize various handcrafted image priors to regularize the solution space. Different from model-driven methods, data-driven methods regard rain removal as a task of learning a non-linear function mapping the observed rainy image into the clean background. Motivated by the unprecedented success of deep learning, they model the mapping function with various convolution neural networks (CNNs). Most of them progressively remove rain streaks via different re-

current neural networks [Li *et al.*, 2018; Ren *et al.*, 2019; Yang and Lu, 2019]. Additionally, adversarial learning-based methods [Zhang *et al.*, 2019] are proposed to prevent derained images from the blur artifact.

However, existing methods suffer from two key limitations despite achieving deraining performance boost. On the one hand, model-driven methods tend to leave some rain streaks or introduce the blur artifact in derained images. This is because physical properties of rain streaks and handcrafted image priors are easily violated on real-world examples where rain streaks are far more complex than modeled. Furthermore, these methods involve heuristic parameter tuning and expensive computation. Data-driven methods, on the other hand, fail to yield plausible rain-free images in an efficient manner (as shown in Fig. 1). Although some lightweight methods [Fan *et al.*, 2018; Fu *et al.*, 2019] have been proposed to improve the computational efficiency, they result in a significant decrease in the deraining performance.

Motivated by addressing above two issues, we propose a residual squeeze-and-excitation network called RSEN for fast image deraining as well as superior deraining performance compared with state-of-the-art approaches. Unlike prevalent recurrent networks reusing flat network structures, RSEN adopts a lightweight encoder-decoder architecture to conduct rain removal in one stage. Besides, both encoder and decoder adopt a novel residual squeeze-and-excitation block as the core of feature extraction, which contains a residual block for producing hierarchical features, followed by a squeeze-and-excitation block for channel-wisely enhancing the resulted hierarchical features.

Main contributions of this paper are listed as follows:

- We propose a novel residual squeeze-and-excitation network called RSEN for image rain removal. It adopts a lightweight encoder-decoder architecture and is capable to effectively remove rain streaks while well preserving texture details.
- We propose to incorporate a residual squeeze-and-excitation block in our network, which can not only generate channel-wisely enhanced hierarchical features but also well benefit gradient propagation.
- Experimental results show that our proposed method can not only considerably reduce the computational complexity but also significantly improve the deraining performance compared with state-of-the-art methods.

The remainder of this paper is organized as follows. Section 2 discusses the related works. Section 3 introduces the proposed network. Then, performance evaluation and comparison are presented in Section 4. Finally, Section 5 concludes the paper and discusses future work.

## 2 Related Work

### 2.1 Image Deraining

Image deraining, a highly ill-posed problem, has drawn increasingly more attention from industry and academia over the past few decades. Existing works can be categorized into two classes, i.e., model-driven methods and data-driven methods.

Model-driven methods can be further divided into filter based ones and prior based ones. Considering rain removal as a task of signal filtering, filter based ones utilize physical properties of rain streaks and edge-preserving filters to obtain rain-free images. Specifically, [Xu *et al.*, 2012] utilize guided filter [He *et al.*, 2010] to remove rain streaks based on the chromatic and brightness property of rain streaks. [Zheng *et al.*, 2013], [Kim *et al.*, 2013], and [Ding *et al.*, 2016] boost the deraining performance via multi-guided filter, non-local means filtering, and guided  $L_0$  smoothing filter, respectively. However, prior based ones formulate rain removal as an optimization problem and employ various handcrafted image priors to regularize the solution space. These image priors include sparse-coding prior [Luo *et al.*, 2015], Gaussian prior [Li *et al.*, 2016] and low-rank prior [Chang *et al.*, 2017].

Different from model-driven methods, data-driven approaches employ various convolution neural networks to automatically learn a non-linear mapping function between the rainy image and the rain-free image from data. More specifically, [Fu *et al.*, 2017a] design a shallow convolution neural network to address rain removal and improve the deraining performance by a deeper network [Fu *et al.*, 2017b]. [Yang *et al.*, 2017] present a multi-task framework, which simultaneously deals with rain detection and rain removal. Unlike one-stage deraining methods, [Li *et al.*, 2018] remove rain streaks stage by stage via a recurrent squeeze-and-excitation context aggregation network. Recently, [Wang *et al.*, 2019] present a spatial attentive single-image deraining approach and [Yang and Lu, 2019] introduce a recurrent hierarchy enhancement network. To preserve more texture details of derained images, adversarial learning-based methods [Zhang *et al.*, 2019] are proposed. In addition, some lightweight methods [Fu *et al.*, 2019; Fan *et al.*, 2018] are dedicated to reduce the computational complexity.

However, existing methods suffer from two key limitations despite achieving deraining performance boost. On the one hand, model-driven methods suffer from under-/over-deraining on real-world examples where rain streaks are far more complex than modeled. On the other hand, existing neural networks fail to produce plausible rain-free images in an efficient manner due to the complex framework. Some lightweight networks attempt to improve computational efficiency but at the cost of obvious performance degradation.

### 2.2 Convolution Neural Network

Recent years have witnessed the convolution neural network goes increasingly deeper (e.g., VGGNet [Simonyan and Zisserman, 2014]). Deep neural networks typically are superior to shallow networks while meeting more challenges in convergence and generalization. To address this problem, [He *et al.*, 2016] first propose residual learning, which can benefit gradient propagation and accelerate convergence. In addition, diverse attention mechanisms are proposed to improve the capability of neural networks, such as channel-wise attention [Hu *et al.*, 2018], self-attention mechanism [Vaswani *et al.*, 2017] and spatial attention [Woo *et al.*, 2018].

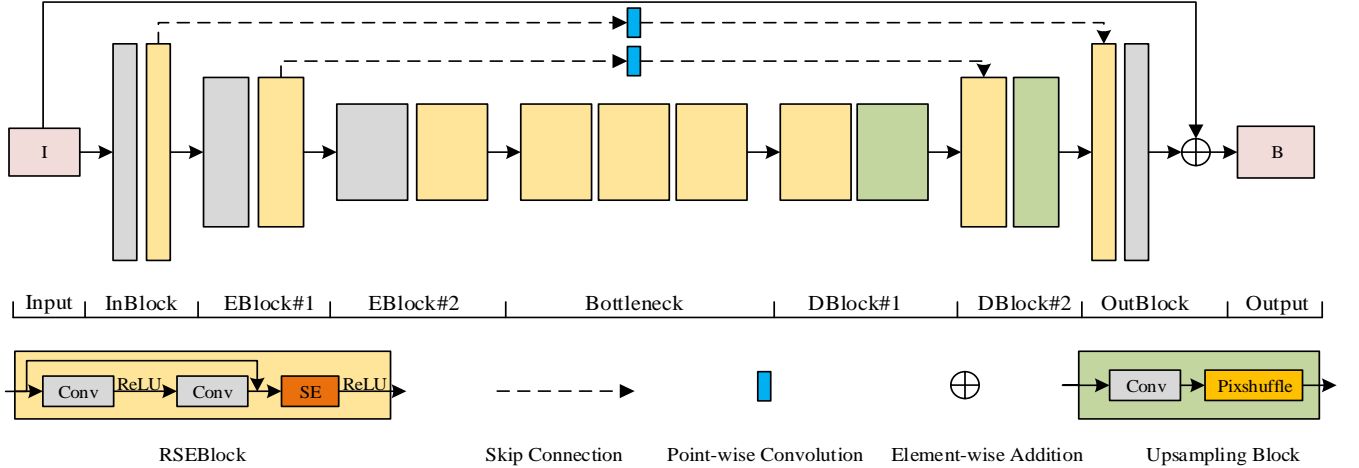


Figure 2: The whole framework of the proposed residual squeeze-and-excitation network. I, B, Conv, and SE represent the input rainy image, the clean background, the conventional convolution and the squeeze-and-excitation block, respectively.

### 3 Proposed Method

#### 3.1 Problem Formulation

Considering rain streak accumulation and overlapping, [Yang *et al.*, 2017] proposes a rain model as follows:

$$I = \alpha(B + \sum_{t=1}^n S_t M) + (1 - \alpha)A, \quad (2)$$

where each  $S_t$  denotes a layer of rain streaks that have the same direction,  $n$  denotes the total number of rain streak layers,  $M$  records the locations of  $S_t$ ,  $A$  represents the global atmospheric light, and  $\alpha$  is the atmospheric transmission.

Unlike the above model requiring rain detection, [Li *et al.*, 2018] present a simpler model, i.e., dividing the captured rainy scene into the combination of several rain streak layers and a rain-free background. Thus, the rain model can be reformulated as follows:

$$I = B + \sum_{t=1}^n R_t, \quad (3)$$

where  $R_t$  and  $n$  represent the  $t$ -th rain streak layer that consists of one kind of rain streaks and the maximum number of rain streak layers, respectively.

In this paper, we further simplify the rain model as follows:

$$I = B + R. \quad (4)$$

As Eq. 4 implied, we can obtain the rain-free background by subtracting rain streaks  $R$  from the rainy image  $I$ . Therefore, we formulate the rain removal as a task of learning a non-linear mapping function between the rainy image and rain streaks. Inspired by the recent success of deep learning, we propose a residual squeeze-and-excitation network call RSEN to model the non-linear mapping function. As illustrated in Fig. 2, RSEN adopts a commonly used encoder-decoder architecture. The detailed design of this architecture is introduced and explained next.

#### 3.2 Residual Squeeze-and-Excitation Network

The encoder-decoder network typically adopts a symmetric convolution neural network architecture composed of an encoder and a decoder. The encoder transforms the input data into feature maps with smaller spatial sizes and more channels while the decoder transforms the resulted feature maps back to the shape of the input. In addition, skip connections are widely used in this architecture because they can aggregate features at multiple levels and accelerate convergence.

Compared with flat architectures, the encoder-decoder network has shown its superiority in many low-level vision tasks, such as image deblurring [Tao *et al.*, 2018] and image inpainting [Nazeri *et al.*, 2019]. However, to accommodate specific tasks, such a network needs to be carefully designed.

For the task of image deraining, we take the following three key aspects into account in our design. First, the receptive field needs to be large enough to handle heavy rain streaks. To this end, a naive approach is to stack more levels or adding more convolution layers at each level for encoder/decoder modules. However, this strategy will result in a sharp increase in computational complexity and parametric size. Furthermore, such a deep neural architecture generally suffers from a low speed of convergence. Second, aside from global skip connections, local skip connections are also beneficial to gradient propagation and accelerate convergence. Third, according to the experimental results of [Li *et al.*, 2018] and [Yang *et al.*, 2017], the channel-wise attention mechanism is a promising alternative to improve the deraining performance.

Based on the aforementioned analysis, we adapt the encoder-decoder network into our task as follows. First, we propose a residual squeeze-and-excitation block (RSEBlock), which contains a residual block for producing hierarchical features via local skip connections, followed by a squeeze-and-excitation block for channel-wisely enhancing the resulted hierarchical features. It is worth noting that we remove the batch normalization [Ioffe and Szegedy, 2015] from the original residual blocks in ResNet [He *et al.*, 2016] accord-

ing to [Tao *et al.*, 2018] and our experimental results. Second, both encoder and decoder employ the RSEBlock as their core of feature extraction instead of conventional convolution layers. Third, considering that the spatial size of the middle feature map needs to be large enough to keep sufficient spatial information for reconstruction, we only stack two levels in the encoder and the decoder. Finally, to enlarge the size of the receptive field, we stack three RSEBlocks after the encoder.

The proposed network can be mathematically expressed as

$$\begin{aligned} f &= \text{Net}_E(I; \theta_E), \\ h &= \text{Net}_B(f; \theta_B), \\ \hat{B} &= I - \text{Net}_D(h; \theta_D), \end{aligned} \quad (5)$$

where  $\text{Net}_E$ ,  $\text{Net}_B$  and  $\text{Net}_D$  are encoder, bottleneck, and decoder CNNs with parameters  $\theta_E$ ,  $\theta_B$  and  $\theta_D$ .  $f$  and  $h$  are the intermediate feature maps.  $\hat{B}$  is the recovered rain-free image.

The implementation details of our proposed RSEN are specified as follows. In our proposed architecture, there are 1 InBlock, 2 EBlocks, followed by 1 Bottleneck, 2 DBlocks, and 1 OutBlock, as illustrated in Fig. 2. InBlock composed of a convolution layer and a RSEBlock transforms the input 3-channel rainy image into a 64-channel feature map. Each EBlock adopts the same structure as InBlock while doubling the number of kernels in the previous layer and downsampling feature maps by half. DBlocks is symmetric to EBlock. It is designed to double the spatial size of feature maps and halve channels, composed of a RSEBlock and a upsampling block. In the upsampling block, a point-wise convolution is used to increase the channel dimension of the input 4 times, followed by a pix-shuffle layer [Shi *et al.*, 2016] whose scale factor is set to 2. Additionally, 2 point-wise convolutions are designed for skip connections. The Bottleneck contains 3 RESBlocks that have the same number of channels. OutBlock takes previous feature maps as input and generates estimated rain streaks. All squeeze-and-excitation blocks squeeze the channel dimension of the input feature map to 6. The stride size for the convolution layer in EBlocks is 2, while all others are 1. Rectified Linear Units (ReLU) are used as the activation function for all layers, and all kernel sizes are set to 3.

### 3.3 Loss Function

The loss function is defined as the mean square error (MSE) between the derained image and its corresponding groundtruth, which can be formulated as follows:

$$L = \frac{1}{2HWC} \sum_i \sum_j \sum_k \|\hat{B}_{i,j,k} - B_{i,j,k}\|_2^2, \quad (6)$$

where  $H$ ,  $W$ , and  $C$  represent the height, width, and channel number of the rain-free image.  $\hat{B}$  and  $B$  denote the restored rain-free image and the groundtruth, respectively.

## 4 Experiments

### 4.1 Dataset and Evaluation Metrics

We choose four synthetic datasets and a real-world dataset for the deraining experiment. The synthetic datasets include

Table 1: Details of synthetic and real-world datasets. Values in each column of the training set and testing set indicate the number of rain-free/rainy image pairs with the exception of the real-world set with rainy images only.

| Datasets       | Training Set | Testing Set | Label              |
|----------------|--------------|-------------|--------------------|
| Rain100H       | 1800         | 100         | rain mask/rain map |
| Rain800        | 700          | 100         | -                  |
| Rain1200       | 12000        | 1200        | rain mask/rain map |
| Rain1400       | 12600        | 1400        | -                  |
| Real-world set | -            | 13          | -                  |

Rain100H, Rain800, Rain1200 and Rain1400. Rain100H is synthesized by [Yang *et al.*, 2017]. Rain800 is obtained from [Zhang *et al.*, 2019]. Rain1200 is provided by [Zhang and Patel, 2018] while Rain1400 comes from [Fu *et al.*, 2017b]. The real-world dataset is constructed by [Yang *et al.*, 2017]. Rainy images in these datasets are diverse in terms of content as well as the type of rain streaks. More details of these datasets are listed in Table 1.

Deraining performances on the synthetic datasets are evaluated in terms of peak signal-to-noise (PSNR) [Huynh-Thu and Ghanbari, 2008] and structural similarity (SSIM) [Wang *et al.*, 2004]. Due to lacking the groundtruth of real-world rainy images, performances of different methods on the real-world dataset are evaluated visually. We compare RSEN with state-of-the-art methods including DSC [Luo *et al.*, 2015], LP [Li *et al.*, 2016], JCAS [Gu *et al.*, 2017], DDN [Fu *et al.*, 2017b], JORDER [Yang *et al.*, 2017], DID-MDN [Zhang and Patel, 2018], DualCNN [Pan *et al.*, 2018], RESCAN [Li *et al.*, 2018], ID\_CGAN [Zhang *et al.*, 2019], ReHEN [Yang and Lu, 2019], SPANET [Wang *et al.*, 2019], and PReNET [Ren *et al.*, 2019].

### 4.2 Training Details

We implement our model using the PyTorch [Paszke *et al.*, 2017] framework. During training, 4 rain-free/rainy patch pairs with a size of  $256 \times 256$  are randomly generated from input image pairs per iteration. All trainable variables of the proposed RSEN are initialized by the default initializer and optimized via the Adam optimizer [Kingma and Ba, 2014].  $\beta_1$ ,  $\beta_2$  and  $\epsilon$  of the Adam optimizer are set to 0.9, 0.999, and  $10^{-8}$  respectively. We train RSEN on a NVIDIA Geforce GTX 1080Ti GPU for 700 epochs. The learning rate is initialized as  $10^{-4}$  and decayed in half every 150 epochs. For fair comparison with existing methods, we only use rain-free/rainy image pairs for training without other additional labels and any data augmentation.

### 4.3 Results on Synthetic Dataset

Table 2 presents quantitative results of different methods on four synthetic datasets. We can observe that the proposed method achieves substantial improvements over state-of-the-art approaches in terms of both PSNR and SSIM. Specifically, the proposed method obtains significant improvements by PSNR of 2.80 dB, 0.62 dB, 0.55 dB, 0.31 dB and SSIM of 0.014, 0.002, 0.09, 0.06 on Rain100H, Rain800, Rain1200, and Rain1400, respectively. Average running time for a

Table 2: Parametric size, running time, and average PSNR and SSIM values on four synthetic datasets. The value with red bold font denotes ranking the first place in this column while value with blue font is the second place. It is worth noting that both PSNR and SSIM are calculated in the RGB color space.

| Methods           | Params    | Time (s) | Rain100H |       | Rain800 |       | Rain1200 |       | Rain1400 |       |
|-------------------|-----------|----------|----------|-------|---------|-------|----------|-------|----------|-------|
|                   |           | 512x512  | PSNR     | SSIM  | PSNR    | SSIM  | PSNR     | SSIM  | PSNR     | SSIM  |
| Rainy             | -         | -        | 12.13    | 0.349 | 21.16   | 0.652 | 21.15    | 0.778 | 23.69    | 0.757 |
| DSC(ICCV'15)      | -         | -        | 15.66    | 0.544 | 18.56   | 0.599 | 21.44    | 0.789 | 22.03    | 0.799 |
| LP(CVPR'16)       | -         | -        | 14.26    | 0.423 | 22.27   | 0.741 | 22.75    | 0.835 | 25.64    | 0.836 |
| JCAS(ICCV'17)     | -         | -        | 13.65    | 0.459 | 22.19   | 0.766 | 27.91    | 0.778 | 28.77    | 0.819 |
| DDN(CVPR'17)      | 57,369    | 0.547    | 24.95    | 0.781 | 21.16   | 0.732 | 27.33    | 0.898 | 27.61    | 0.901 |
| JORDER(CVPR'17)   | 369,792   | 0.268    | 22.15    | 0.674 | 22.24   | 0.776 | 24.32    | 0.862 | 27.55    | 0.853 |
| DID-MDN(CVPR'18)  | 372,839   | 0.532    | 17.39    | 0.612 | 21.89   | 0.795 | 27.95    | 0.908 | 27.99    | 0.869 |
| DualCNN(CVPR'18)  | 687,008   | 20.19    | 14.23    | 0.468 | 24.11   | 0.821 | 23.38    | 0.787 | 24.98    | 0.838 |
| RESCAN(ECCV'18)   | 134,424   | 0.281    | 26.45    | 0.846 | 24.09   | 0.841 | 29.95    | 0.884 | 28.57    | 0.891 |
| ID_CGAN(TCSVT'19) | 817,824   | 0.286    | 14.16    | 0.607 | 22.73   | 0.817 | 23.32    | 0.803 | 21.93    | 0.784 |
| ReHEN(MM'19)      | 298,263   | 0.181    | 27.97    | 0.864 | 26.96   | 0.854 | 32.64    | 0.914 | 31.33    | 0.918 |
| SPANet(CVPR'19)   | 283,716   | 2.301    | -        | -     | -       | -     | 28.64    | 0.91  | -        | -     |
| PReNET(CVPR'19)   | 168,693   | 0.461    | 28.06    | 0.888 | -       | -     | -        | -     | 30.73    | 0.918 |
| Ours              | 4,851,373 | 0.040    | 30.86    | 0.902 | 27.58   | 0.856 | 33.19    | 0.923 | 31.64    | 0.924 |

Table 3: Ablation study on different modules of the proposed RSEN. The CoarseNet denotes the architecture without any enhancement tricks.

| Method                      | Rain100H |       | Rain800 |       | Rain1200 |       | Rain1400 |       |
|-----------------------------|----------|-------|---------|-------|----------|-------|----------|-------|
|                             | PSNR     | SSIM  | PSNR    | SSIM  | PSNR     | SSIM  | PSNR     | SSIM  |
| CoarseNet                   | 28.28    | 0.822 | 21.42   | 0.647 | 32.64    | 0.908 | 31.36    | 0.917 |
| CoarseNet + Skip            | 30.02    | 0.888 | 26.47   | 0.845 | 32.88    | 0.919 | 31.45    | 0.922 |
| CoarseNet + Skip + RES      | 30.86    | 0.902 | 26.90   | 0.854 | 33.11    | 0.923 | 31.54    | 0.924 |
| CoarseNet + Skip + RES + SE | 30.30    | 0.893 | 27.58   | 0.856 | 33.19    | 0.923 | 31.64    | 0.924 |

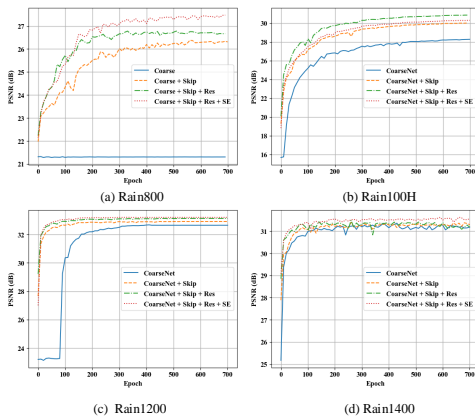


Figure 3: Training convergence analysis on PSNR of RSEN with different modules.

rainy image with a size of  $512 \times 512$  and the parametric size of each method are also chosen for comparison. It can be observed that the proposed method significantly reduces the computational complexity in spite of using relatively more parameters compared with other methods. For instance, RSEN reaches around 4, 10 and 50 times faster than ReHEN, PReNET, and SPANet, respectively. This confirms the superiority of our proposed architecture.

Fig. 4 visually compares the proposed method with three

recent state-of-the-art methods. We can observe that the proposed method achieves the best visual quality. Specifically, compared with other methods, our proposed method avoids leaving obvious artifacts (e.g., rain streaks and the blur artifact) in derained images as well as preserving more structural information.

#### 4.4 Results on Real-World Dataset

To assess the generalization of the proposed method, we also evaluate the proposed method on a real-world dataset. For fair comparison, all the methods employ the pre-trained model trained on the Rain100H dataset to remove rain streaks from real-world rainy images. As demonstrated in Fig. 5, the proposed method produces more natural and pleasant derained images compared with four state-of-the-art methods. Specifically, in our experiment, DDN fails to remove rain streaks from real-world rainy images in most cases while JORDER is prone to dim and blur the details of the derained results. Compared with PReNET and ReHEN, the proposed method can more effectively remove rain streaks from real-world rainy images and restore more texture details.

#### 4.5 Ablation Study

Table 3 and Fig. 3 show the ablation investigation on the effects of the skip connection (SKip), the residual connection (RES), and the squeeze-and-excitation block (SE). As can be observed, both Skip and RES are beneficial for convergence and boosting deraining performance. Specifically, the



Figure 4: Derained results of RESCAN, JORDER, PReNET, and the proposed method on synthetic rainy images.

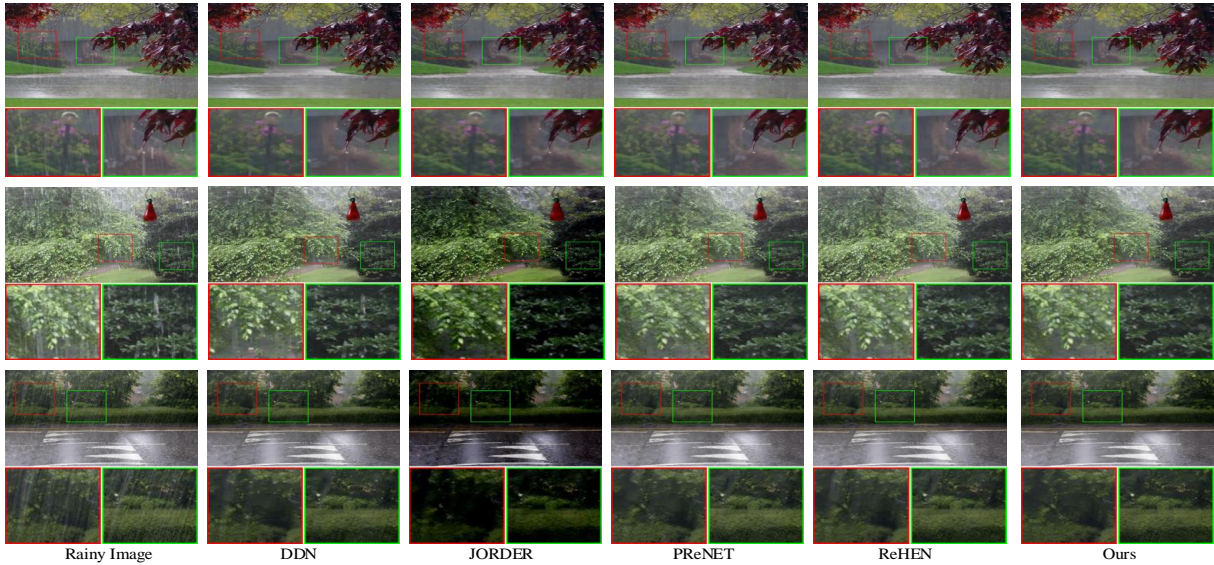


Figure 5: Derained results of DDN, JORDER, PReNET, ReHEN, and the proposed method on real-world rainy images.

Skip brings gains by PSNR of 1.74 dB, 5.02 dB, 0.24 dB and 0.09 dB on Rain100H, Rain800, Rain1200, and Rain1400, respectively, while the RES obtains 0.84 dB, 0.43 dB, 0.23 dB, and 0.09 dB gains. The SE is useful for most datasets except for Rain100H. This may be because synthesized rainy images with five streak directions in Rain100H are more complex than other datasets with one streak direction. Hence, we disable the SE in all the RSEBlocks when performing rain removal on Rain100H.

## 5 Conclusion

In this paper, we propose a novel residual squeeze-and-excitation network called RSEN for fast image deraining as

well as superior deraining performance compared with existing approaches. Specifically, RSEN adopts a lightweight encoder-decoder architecture to conduct rain removal in one stage. Besides, both encoder and decoder adopt a novel residual squeeze-and-excitation block as the core of feature extraction, where a residual block and a squeeze-and-excitation block are used to produce and channel-wisely enhance hierarchical features, respectively. Experimental results demonstrate that our method can not only considerably reduce the computational complexity but also achieve significant improvements in the deraining performance compared with state-of-the-art methods. In the future, we plan to extend our work to deal with video deraining, e.g., incorporating an extra module in our network to capture temporal information.

## References

- [Chang *et al.*, 2017] Yi Chang, Luxin Yan, and Sheng Zhong. Transformed low-rank model for line pattern noise removal. In *Proceedings of the IEEE International Conference on Computer Vision*, pages 1726–1734, 2017.
- [Ding *et al.*, 2016] Xinghao Ding, Liqin Chen, Xianhui Zheng, Yue Huang, and Delu Zeng. Single image rain and snow removal via guided l0 smoothing filter. *Multimedia Tools and Applications*, 75(5):2697–2712, 2016.
- [Fan *et al.*, 2018] Zhiwen Fan, Huaifeng Wu, Xueyang Fu, Yue Huang, and Xinghao Ding. Residual-guide feature fusion network for single image deraining. *arXiv preprint arXiv:1804.07493*, 2018.
- [Fu *et al.*, 2017a] Xueyang Fu, Jiabin Huang, Xinghao Ding, Yinghao Liao, and John Paisley. Clearing the skies: A deep network architecture for single-image rain removal. *IEEE Transactions on Image Processing*, 26(6):2944–2956, 2017.
- [Fu *et al.*, 2017b] Xueyang Fu, Jiabin Huang, Delu Zeng, Yue Huang, Xinghao Ding, and John Paisley. Removing rain from single images via a deep detail network. In *Proceedings of the IEEE Conference on Computer Vision and Pattern Recognition*, pages 3855–3863, 2017.
- [Fu *et al.*, 2019] Xueyang Fu, Borong Liang, Yue Huang, Xinghao Ding, and John Paisley. Lightweight pyramid networks for image deraining. *IEEE transactions on neural networks and learning systems*, 2019.
- [Gu *et al.*, 2017] Shuhang Gu, Deyu Meng, Wangmeng Zuo, and Lei Zhang. Joint convolutional analysis and synthesis sparse representation for single image layer separation. In *Proceedings of the IEEE International Conference on Computer Vision*, pages 1708–1716, 2017.
- [He *et al.*, 2010] Kaiming He, Jian Sun, and Xiaoou Tang. Guided image filtering. In *European conference on computer vision*, pages 1–14. Springer, 2010.
- [He *et al.*, 2016] Kaiming He, Xiangyu Zhang, Shaoqing Ren, and Jian Sun. Deep residual learning for image recognition. In *Proceedings of the IEEE conference on computer vision and pattern recognition*, pages 770–778, 2016.
- [Hu *et al.*, 2018] Jie Hu, Li Shen, and Gang Sun. Squeeze-and-excitation networks. In *Proceedings of the IEEE conference on computer vision and pattern recognition*, pages 7132–7141, 2018.
- [Huynh-Thu and Ghanbari, 2008] Quan Huynh-Thu and Mohammed Ghanbari. Scope of validity of psnr in image/video quality assessment. *Electronics letters*, 44(13):800–801, 2008.
- [Ioffe and Szegedy, 2015] Sergey Ioffe and Christian Szegedy. Batch normalization: Accelerating deep network training by reducing internal covariate shift. *arXiv preprint arXiv:1502.03167*, 2015.
- [Kim *et al.*, 2013] Jin-Hwan Kim, Chul Lee, Jae-Young Sim, and Chang-Su Kim. Single-image deraining using an adaptive nonlocal means filter. In *2013 IEEE International Conference on Image Processing*, pages 914–917. IEEE, 2013.
- [Kingma and Ba, 2014] Diederik P Kingma and Jimmy Ba. Adam: A method for stochastic optimization. *arXiv preprint arXiv:1412.6980*, 2014.
- [Li *et al.*, 2016] Yu Li, Robby T Tan, Xiaojie Guo, Jiangbo Lu, and Michael S Brown. Rain streak removal using layer priors. In *Proceedings of the IEEE conference on computer vision and pattern recognition*, pages 2736–2744, 2016.
- [Li *et al.*, 2018] Xia Li, Jianlong Wu, Zhouchen Lin, Hong Liu, and Hongbin Zha. Recurrent squeeze-and-excitation context aggregation net for single image deraining. In *Proceedings of the European Conference on Computer Vision (ECCV)*, pages 254–269, 2018.
- [Liu *et al.*, 2019] Wei Liu, Shengcai Liao, Weiqiang Ren, Weidong Hu, and Yanan Yu. High-level semantic feature detection: A new perspective for pedestrian detection. In *Proceedings of the IEEE Conference on Computer Vision and Pattern Recognition*, pages 5187–5196, 2019.
- [Luo *et al.*, 2015] Yu Luo, Yong Xu, and Hui Ji. Removing rain from a single image via discriminative sparse coding. In *Proceedings of the IEEE International Conference on Computer Vision*, pages 3397–3405, 2015.
- [Nazeri *et al.*, 2019] Kamyar Nazeri, Eric Ng, Tony Joseph, Faisal Qureshi, and Mehran Ebrahimi. Edgeconnect: Generative image inpainting with adversarial edge learning. *arXiv preprint arXiv:1901.00212*, 2019.
- [Pan *et al.*, 2018] Jinshan Pan, Sifei Liu, Deqing Sun, Jiawei Zhang, Yang Liu, Jimmy Ren, Zechao Li, Jinhui Tang, Huchuan Lu, Yu-Wing Tai, et al. Learning dual convolutional neural networks for low-level vision. In *Proceedings of the IEEE conference on computer vision and pattern recognition*, pages 3070–3079, 2018.
- [Paszke *et al.*, 2017] Adam Paszke, Sam Gross, Soumith Chintala, Gregory Chanan, Edward Yang, Zachary DeVito, Zeming Lin, Alban Desmaison, Luca Antiga, and Adam Lerer. Automatic differentiation in pytorch. 2017.
- [Redmon and Farhadi, 2018] Joseph Redmon and Ali Farhadi. Yolov3: An incremental improvement. *arXiv preprint arXiv:1804.02767*, 2018.
- [Ren *et al.*, 2019] Dongwei Ren, Wangmeng Zuo, Qinghua Hu, Pengfei Zhu, and Deyu Meng. Progressive image deraining networks: a better and simpler baseline. In *Proceedings of the IEEE Conference on Computer Vision and Pattern Recognition*, pages 3937–3946, 2019.
- [Shi *et al.*, 2016] Wenzhe Shi, Jose Caballero, Ferenc Huszár, Johannes Totz, Andrew P Aitken, Rob Bishop, Daniel Rueckert, and Zehan Wang. Real-time single image and video super-resolution using an efficient sub-pixel convolutional neural network. In *Proceedings of the IEEE conference on computer vision and pattern recognition*, pages 1874–1883, 2016.
- [Simonyan and Zisserman, 2014] Karen Simonyan and Andrew Zisserman. Very deep convolutional networks for large-scale image recognition. *arXiv preprint arXiv:1409.1556*, 2014.
- [Tao *et al.*, 2018] Xin Tao, Hongyun Gao, Xiaoyong Shen, Jue Wang, and Jiaya Jia. Scale-recurrent network for deep image deblurring. In *Proceedings of the IEEE Conference on Computer Vision and Pattern Recognition*, pages 8174–8182, 2018.
- [Vaswani *et al.*, 2017] Ashish Vaswani, Noam Shazeer, Niki Parmar, Jakob Uszkoreit, Llion Jones, Aidan N Gomez, Łukasz Kaiser, and Illia Polosukhin. Attention is all you need. In *Advances in neural information processing systems*, pages 5998–6008, 2017.
- [Wang *et al.*, 2004] Zhou Wang, Alan C Bovik, Hamid R Sheikh, Eero P Simoncelli, et al. Image quality assessment: from error visibility to structural similarity. *IEEE transactions on image processing*, 13(4):600–612, 2004.
- [Wang *et al.*, 2019] Tianyu Wang, Xin Yang, Ke Xu, Shaozhe Chen, Qiang Zhang, and Rynson WH Lau. Spatial attentive single-image deraining with a high quality real rain dataset. In *Proceedings of the IEEE Conference on Computer Vision and Pattern Recognition*, pages 12270–12279, 2019.
- [Woo *et al.*, 2018] Sanghyun Woo, Jongchan Park, Joon-Young Lee, and In So Kweon. Cbam: Convolutional block attention module. In *Proceedings of the European Conference on Computer Vision (ECCV)*, pages 3–19, 2018.
- [Xu *et al.*, 2012] Jing Xu, Wei Zhao, Peng Liu, and Xianglong Tang. Removing rain and snow in a single image using guided filter. In *2012 IEEE International Conference on Computer Science and Automation Engineering (CSAE)*, volume 2, pages 304–307. IEEE, 2012.
- [Yang and Lu, 2019] Youzhao Yang and Hong Lu. Single image deraining via recurrent hierarchy enhancement network. In *Proceedings of the 27th ACM International Conference on Multimedia*, pages 1814–1822. ACM, 2019.
- [Yang *et al.*, 2017] Wenhan Yang, Robby T Tan, Jiashi Feng, Jiaying Liu, Zongming Guo, and Shuicheng Yan. Deep joint rain detection and removal from a single image. In *Proceedings of the IEEE Conference on Computer Vision and Pattern Recognition*, pages 1357–1366, 2017.
- [Zang *et al.*, 2019] Shizhe Zang, Ming Ding, David Smith, Paul Tyler, Thierry Rakotariovelo, and Mohamed Ali Kaafar. The impact of adverse weather conditions on autonomous vehicles: How rain, snow, fog, and hail affect the performance of a self-driving car. *IEEE Vehicular Technology Magazine*, 14(2):103–111, 2019.
- [Zhang and Patel, 2018] He Zhang and Vishal M Patel. Density-aware single image de-raining using a multi-stream dense network. In *Proceedings of the IEEE conference on computer vision and pattern recognition*, pages 695–704, 2018.
- [Zhang *et al.*, 2019] He Zhang, Vishwanath Sindagi, and Vishal M Patel. Image deraining using a conditional generative adversarial network. *IEEE transactions on circuits and systems for video technology*, 2019.
- [Zheng *et al.*, 2013] Xianhui Zheng, Yinghao Liao, Wei Guo, Xueyang Fu, and Xinghao Ding. Single-image-based rain and snow removal using multi-guided filter. In *International Conference on Neural Information Processing*, pages 258–265. Springer, 2013.